Elastic flow-front fingering instability in flowing polymer solutions

Kabanemi, Kalonji K.; Hétu, Jean-François; Sammoun, Samira H.

Publisher's version / la version de l'éditeur:
Rheologica Acta, 45, 5, pp. 693-704

Web page / page Web
http://dx.doi.org/10.1007/s00397-005-0027-5
http://nparc.cisti-icist.nrc-cnrc.gc.ca/npsi/ctrl?action=rtdoc&an=15861571&lang=en
http://nparc.cisti-icist.nrc-cnrc.gc.ca/npsi/ctrl?action=rtdoc&an=15861571&lang=fr

Rheol Acta (2006) 45: 693–704
DOI 10.1007/s00397-005-0027-5

ORIGINAL CONTRIBUTION

Kalonji K. Kabanemi
Jean-François Hétu
Samira H. Sammoun

Elastic flow-front fingering instability in flowing polymer solutions

Received: 13 July 2005
Accepted: 25 July 2005
Published online: 15 September 2005

K. K. Kabanemi (✉) · J.-F. Hétu
S. H. Sammoun
Industrial Materials Institute,
National Research Council of Canada,
75, de Mortagne, Boucherville,
QC, J4B 6Y4, Canada
E-mail: kalonji.kabanemi@cnrc-nrc.gc.ca

Abstract An experimental investigation of the flow-front behavior of dilute and semi-dilute polymer solutions has been carried out to gain a better understanding of the underlying mechanisms leading to the occurrence of an unstable flow at the advancing flow-front during the filling of a rectangular Hele-Shaw cell. Our experimental results have revealed the existence of an elastic finger-like instability at the advancing flow-front that develops in semi-dilute solutions of high molecular weight polymers, with an onset time of approximately a few hundred milliseconds. Although at shear rates above critical, narrow finger patterns develop at the flow-front, their amplitude and number remain roughly constant throughout the flowing. At critical condition, no secondary flow was observed in the vicinity of the front region where the unstable flow develops. Transient response of the normal stress difference and the shear stress in the plate-and-plate geometry at shear rate above critical (for the elastic fingering instability in the Hele-Shaw cell) did not reveal any anomalous that could lead to the formation of such finger-like instabilities. These instabilities were observed for both the ideal elastic Boger fluids and shear thinning viscoelastic fluids.

Keywords Elastic instability · Flow-front instability · Viscous instability · Fingering instability · Finger patterns · Injection molding

Introduction

The occurrence of instabilities during the processing of a polymer melt has challenged the polymer processing community for years. Different types of instabilities, such as purely elastic instability in Taylor-Couette flows (Jackson et al. 1984; Magda and Larson 1988; McKinley et al. 1991; Larson 1992), Saffman-Taylor instabilities (Kondic et al. 1998; Linder et al. 2000, 2002; Fast et al. 2001) or stick-slip related extrusion instabilities (Petrie and Denn 1976; Denn 2001), have been observed and studied in the past. In the present work, we are concerned only with fingering instabilities that develop at an advancing flow-front in an empty mold cavity (only one fluid flowing in the cavity). A schematic view of the problem is shown in Fig. 1. In our experiments, the polymer first flows in a cylindrical or rectangular duct and then enters into an empty rectangular Hele-Shaw cell (mold cavity). The mold is designed such that the air in the cavity is continuously evacuated to avoid any flow-front viscous instability that may be caused by the compressed air in the cavity. Thus, throughout the filling of the cavity, for reasons discussed below, an unstable flow develops at the front, leading to the formation of finger-like patterns whose amplitude remain roughly constant in the course of filling.

The fingering instability at the advancing flow-front reported in the present work differs from the other

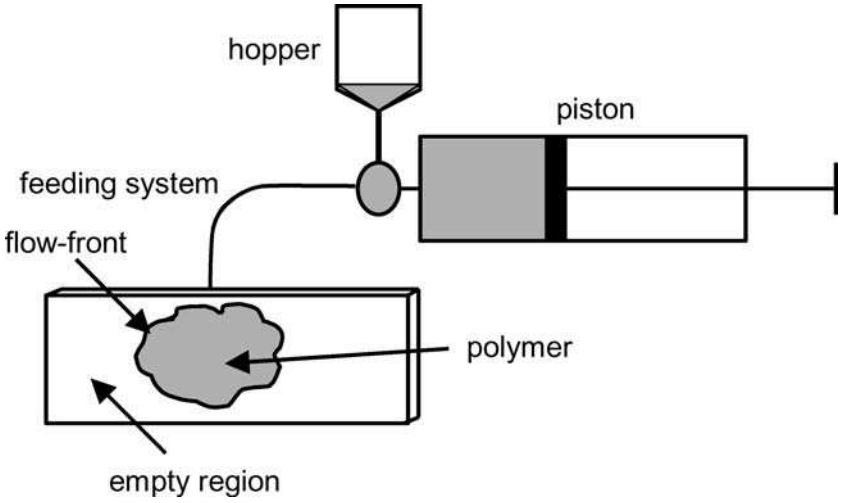

Fig. 1 Schematic diagram of the system used for flow visualization. The view direction is normal to the middle-plane of the cavity

instabilities mentioned before. The purely elastic instability reported by Jackson et al. (1984), Magda and Larson (1988), McKinley et al. (1991) and Larson (1992) occurs in Taylor-Couette, cone-and-plate and parallel-plate flows, above a critical shear rate. This elastic instability manifests itself after a long shearing experiment where a time-dependent increase in shear viscosity and elasticity or anti-thixotropic behavior is observed. The induction time for the onset of this instability ranges from several minutes to a few seconds and is a very sensitive function of the Deborah number, De. McKinley et al. (1991) concluded that such a behavior seems to result from a kinematic transition from a simple viscometric flow to a time-dependent state consisting of a tangential shear flow and a nonaxisymmetric, secondary flow. On the other hand, the Saffman-Taylor instability (viscous instability) occurs when a low viscosity fluid is injected into a more viscous one. An unstable chaotic or fractal pattern results. Saffman-Taylor instabilities appear in many diverse injection-molding processes including the gas-assisted or co-injection. An extensive literature review of theory and experiments, that deal with this issue may be found in Kondic et al. (1998), Linder et al. (2000), Fast et al. (2001) and Linder et al. (2002), among others. The flow-front instability reported in this paper is also quite different from stick-slip extrusion instability (see, e.g., Petrie and Denn 1976; Denn 2001).

Quite a few theories have been reported or proposed to elucidate fingering instabilities. While extensive work exists that deal with purely elastic or viscous instabilities (see, e.g., Jackson et al. 1984; Magda and Larson 1988; Larson et al. 1990; McKinley et al. 1991; Larson 1992; Kondic et al. 1998; Linder et al. 2000, 2002; Fast et al. 2001), to our knowledge, no study exists that deal with the elastic fingering instability, that occurs at an advancing flow-front of polymer solutions, during flowing in an empty mold cavity. A preliminary experimental study on mold filling by Kabanemi and Gobeaux (1987), using a well-characterized polymer solution consisting of 0.1% by weight of polyisobutylene, 92.1% of polybutene (PB) and 7.8% of kerosene, revealed anomalous flow-front distortions during filling and the occurrence of finger-like instabilities at the advancing flow-front. We decided to investigate this issue in greater detail.

The primary purpose of this work is to study the mechanism of flow-front fingering instabilities during flowing of dilute and semi-dilute polymer solutions in a rectangular Hele-Shaw cell. Our experimental investigations focus on two different classes of fluids, i.e., ideal elastic Boger fluids [polyacrylamide (PAA) and polyisobutylene (PIB) solutions], and shear thinning viscoelastic fluids. Numerous factors that could influence the occurrence of such flow-front fingering instabilities are investigated including the shear rate, the molecular weight and the polymer concentration. The rest of the paper is organized as follows. First, the experimental apparatus, the solution preparation and the methodology are presented. Second, the description of experiments along with experimental observations is discussed to understand the mechanism that leads to the occurrence of flow-front fingering instabilities.

Experimental setup and solution preparation

The experimental setup is described in the schematic in Fig. 1. The polymer solutions were injected in the cavity by using a piston system. A laser sheet lighting was used to illuminate plane of polymer solution at different locations across the cavity thickness. This enabled us to track seeding particles during flowing and to analyze in-depth flow behavior in the front region. A camera was connected to a monitor to record the sequence of flow-front patterns in the course of filling. The flow rate and the pressure were recorded simultaneously during filling.

Two different polymers were used in this study. The first polymer used was a PAA from Scientific Polymer Products. It has either a high molecular weight of 5–6×10^6 g mole^{-1} or a low molecular weight of 10^4 g mole^{-1}. The solvent consisted in a mixture of water and corn syrup (Clearsweet 63/43 IX from Cargill Sweeteners). Different solutions were designed to study the effect of concentration and molecular weight on the flow-front shape. These are described along with the experimental results in the following section. To design the sample, first a master solution of PAA was dissolved in distilled water, because PAA is very hard to dissolve in corn syrup. After the master solution has been prepared, it was mixed with the corn syrup progressively until a homogeneous solution was obtained. Polymer solutions above 1% by weight concentration were mixed for days to ensure complete dissolution.

To rule out any physical conjectures regarding the solution preparation, i.e., a possible poorly mixed solutions, and to describe the real physics of such solutions, the results of a well-characterized Boger fluid, consisting of 0.1% by weight of PIB (10^6 g mole^{-1}, MML-120), 92.1% of PB (HYVIS 10) and 7.8% of kerosene (Kabanemi and Gobeaux 1987), were compared to those for the PAA Boger fluid, to demonstrate the validity of our experimental observations.

Experimental observations and rheological measurements

Flow visualization experiments were designed to analyze flow-front fingering instabilities that occur during flowing of polymer solutions in a 150 mm × 60 mm rectangular Hele-Shaw cell with a 3 mm gap (cavity thickness). Injected fluids were either PAA-based solutions or PIB-based solutions. The temperature of solutions was constant (about 23 °C) and the flow rate was kept fixed during each filling experiment.

The solutions were characterized in a controlled stress environment using the Rheometrics Dynamic Stress Rheometer SR-200 at 23 °C, equipped with the 50 mm diameter parallel plates geometry. Both dynamic and steady shear experiments were carried out. The steady state shear viscosity was measured as a function of the shear rate along with corresponding shear stress and first normal stress difference in start-up of steady shear flow experiments.

Highly dilute PAA solution

In order to emphasize the major consequences of the polymer mass concentration and the molecular weight on the occurrence of the flow-front instabilities, we first studied the flow behavior of a highly dilute polymer solution (a nearly inelastic fluid) consisting of 0.015% by weight of a high molecular weight PAA (5–6×10^6 g mole^{-1}), in the mixture of corn syrup (95%) and water (5%). The solution is below the rough estimate of the overlap concentration, $c^* = 0.11\%$.

The rheological characterization of the solution in oscillatory shear showing the dynamic viscosity, η^*, the storage modulus, G', and the loss modulus, G'', is presented in Fig. 2. It can be seen that, at this very low concentration, the fluid behaves as a Newtonian fluid, with almost no measurable normal stress for the shear rates investigated in our filling experiments. Figure 3

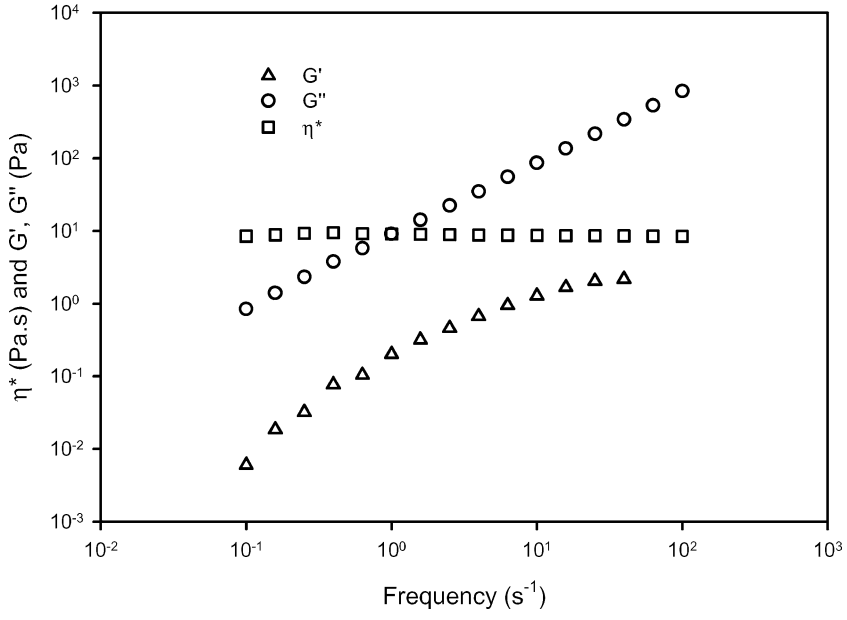

Fig. 2 Complex viscosity, η^*, storage modulus, G', and loss modulus, G'', as a function of frequency at 23 °C for the 0.015% by weight solution of PAA (5–6×10^6 g mole^{-1}), in the mixture of corn syrup (95%) and water (5%)

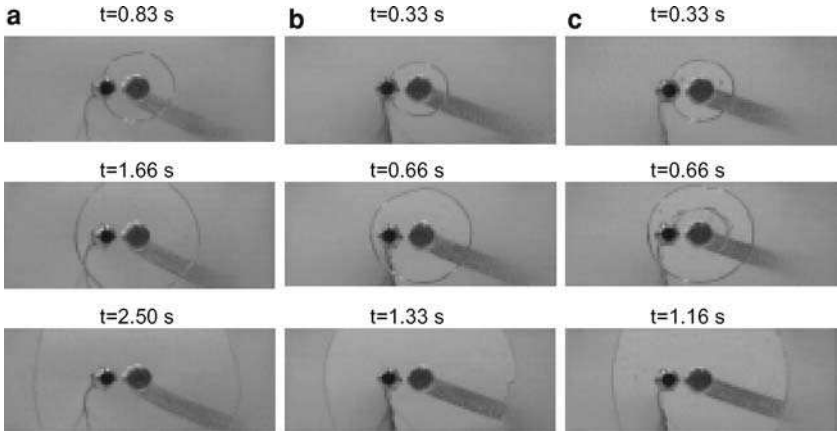

Fig. 3 Effect of the injection flow rate, Q, on the flow-front shape during filling for the 0.015% by weight solution of PAA ($5–6\times10^6$ g mole^{-1}), in the mixture of corn syrup (95%) and water (5%): **a** $Q = 9.6$ cm^3 s^{-1}, **b** $Q = 16.2$ cm^3 s^{-1}, and **c** $Q = 18$ cm^3 s^{-1}

shows flow-front patterns at different time during the cavity filling, at three different flow rate levels. Since the elastic effect is negligibly small in that solution, the flow-front remains smooth throughout the filling and no distortion of the flow-front shape is observed in the range of the flow rate investigated.

PAA and PIB Boger fluids

The second set of experiments was intended for illustrating the polymer contribution on the flow-front behavior and to study the effect of the normal stress difference. The polymer mass concentration of PAA was therefore increased from 0.015% to 0.1%, around the overlap concentration ($c^* = 0.11\%$), in the same mixture of corn syrup (95%) and water (5%). We anticipate that at this concentration the polymer coils come closer and start to overlap each other. So that the experimental observations presented for the PAA Boger fluid bellow are in the semi-dilute regime.

The rheological characterizations of the PAA and PIB Boger fluids used in the filling experiments are shown in Figs. 4, 5, 6, 7, 8. It can be seen from Fig. 4 that these solutions do not shear thin in viscosity over a wide range of the shear rate. The results for the storage modulus, G', and the loss modulus, G'', in oscillatory shear are presented in Fig. 5. It can be seen from this figure that the two Boger fluids exhibit almost the same behavior. Figures 6 and 7 show the shear stress and normal stress difference, N_1, upon the inception of steady shear flow. The effects of the normal stress difference, N_1, are large compared to those for the 0.015% PAA solution displayed by G', and shown in Fig. 2. The

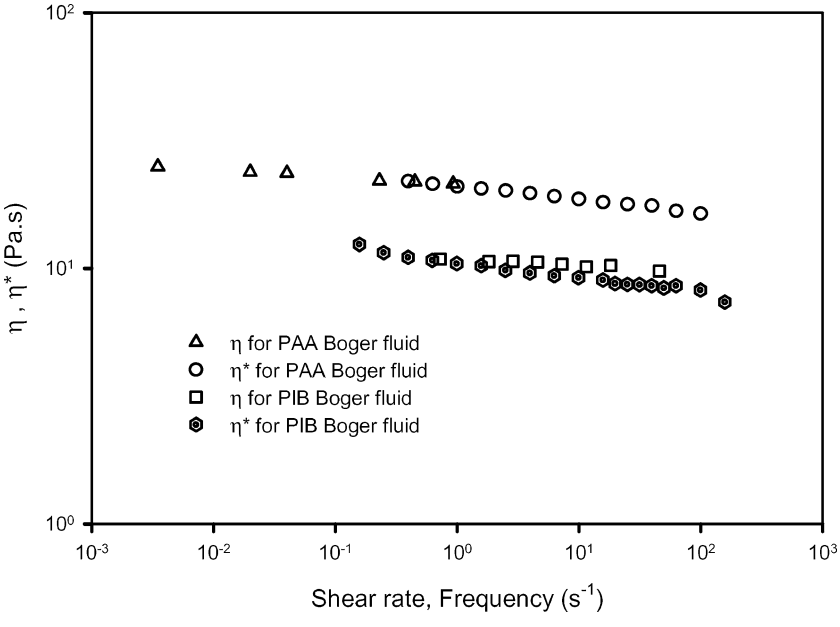

Fig. 4 Shear viscosity, η, and complex viscosity, η^*, for two Boger fluids at 23 °C: **a** 0.1% by weight solution of PAA in the mixture of corn syrup (95%) and water (5%), and **b** 0.1% by weight solution of PIB in the mixture of PB (92.1%) and kerosene (7.8%)

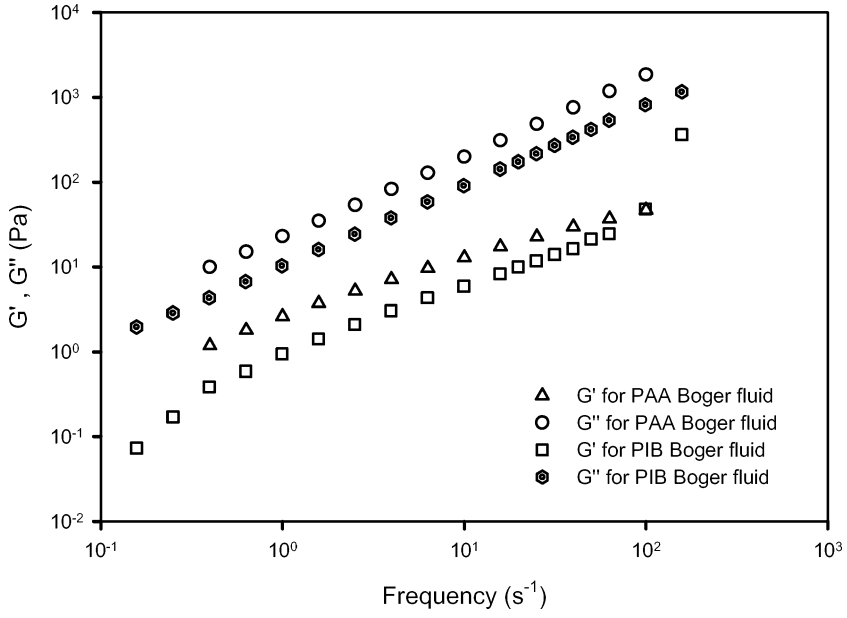

Fig. 5 Storage and loss moduli, G' and G'', as a function of frequency at 23 °C for two Boger fluids: **a** 0.1% by weight solution of PAA in the mixture of corn syrup (95%) and water (5%), and **b** 0.1% by weight solution of PIB in the mixture of PB (92.1%) and kerosene (7.8%)

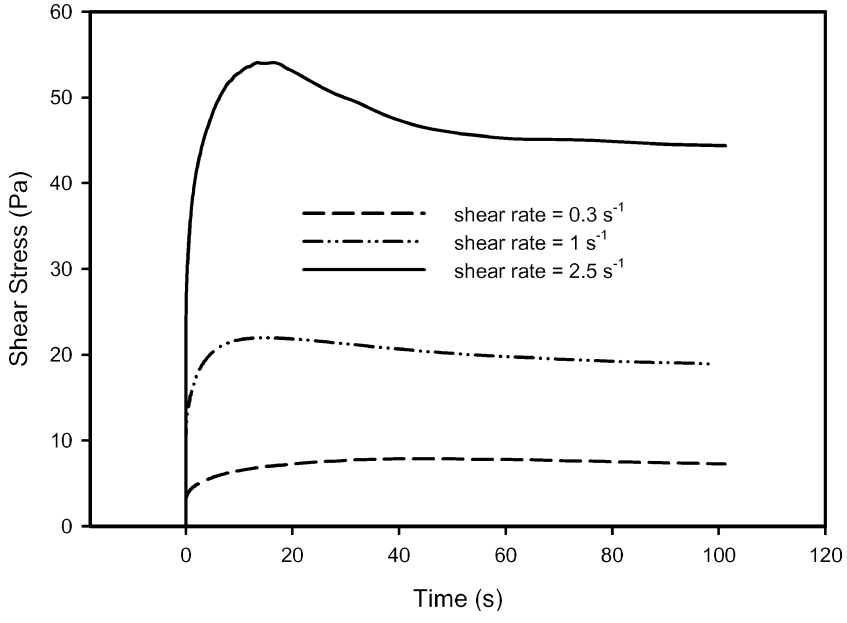

Fig. 6 Time dependence of the shear stress in the plate-and-plate geometry at three different shear rates for the PAA Boger fluid: 0.1% by weight solution of PAA in the mixture of corn syrup (95%) and water (5%)

polymeric relaxation time, λ_p, for the 0.1% PAA Boger fluid has been determined from measurements of the normal stress decay on cessation of steady shear flow. The normal stress relaxation curve is shown in Fig. 8 that yields an estimate of $\lambda_p = 70$ s upon cessation of steady shear flow at shear rate $\dot{\gamma} = 2.5\,\mathrm{s}^{-1}$. We recall that a better characterization is obtained by using a spectrum of relaxation times.

On the basis of the above rheological characterization, a series of flow experiments in the rectangular Hele-Shaw cell was conducted to study the effects of elasticity on the flow-front behavior for the 0.1% PAA Boger fluid. The main observation from these experiments is the deep influence of the concentration on the flow-front shape. Contrary to the flow-front shape of Fig. 9a for the 0.015% PAA solution (nearly inelastic fluid), a deviation from homogeneous smooth flow-front pattern is clearly observed in Figs. 9b, c, where an unstable flow develops at the front region, with the flow-front pattern exhibiting finger-like instabilities. By analyzing the filling sequences in greater detail in Fig. 10, we observe that at the earlier stage of filling, the flow-front pattern is smooth. A few hundred milliseconds later, about 300 ms, macroscopic observable fluctuations of the front

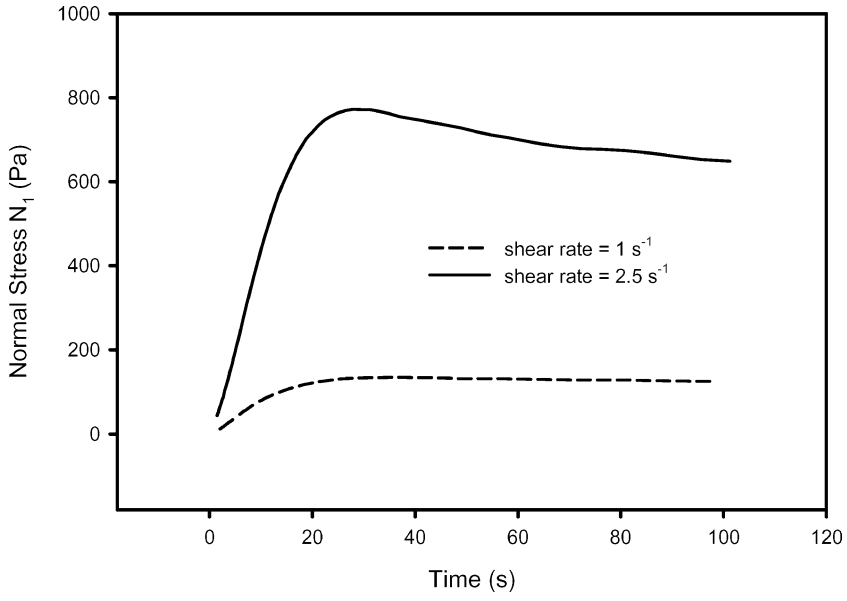

Fig. 7 Time dependence of the normal stress, N_1, in the plate-and-plate geometry at two different shear rates for the PAA Boger fluid: 0.1% by weight solution of PAA in the mixture of corn syrup (95%) and water (5%)

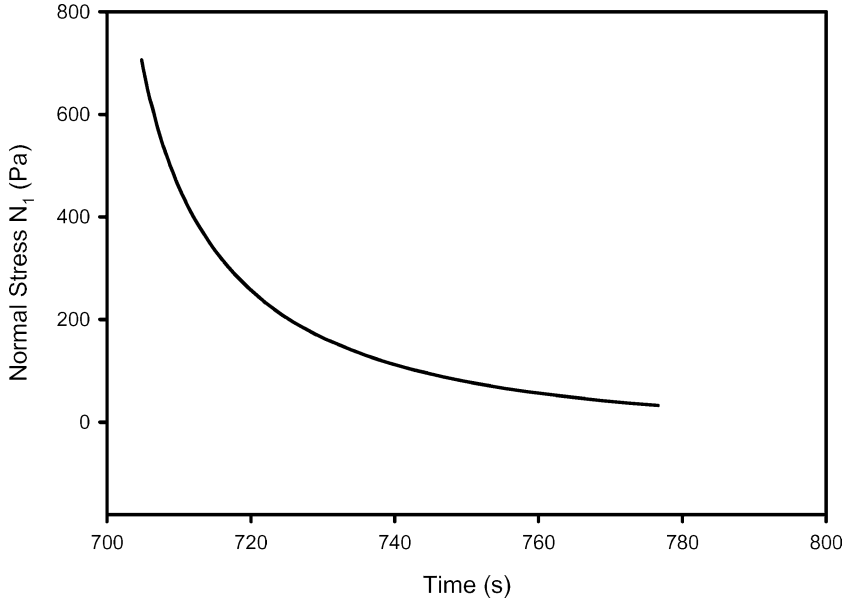

Fig. 8 Normal stress relaxation for the 0.1% PAA Boger fluid upon cessation of steady shear flow at shear rate $\dot{\gamma} = 2.5\,\mathrm{s}^{-1}$

or fingering instabilities develop. It can also be seen from this figure that the unstable flow that develops at the advancing flow is not chaotic, and the amplitude and number of fingers remain roughly constant throughout the filling.

In order to examine the flow-front shape in the front region more closely, across the cavity thickness, we have used a laser sheet lighting to illuminate plane of polymer solution at different locations across the cavity thickness. As can be seen from Fig. 11b, contrary to the flow-front shape in the middle plane direction that exhibits inhomogeneous deformations (Fig. 11a), the flow-front shape does not exhibit any macroscopic observable finger-like pattern in the gap-wise direction (Fig. 11b). In addition, our experimental observations using the laser sheet did not reveal the existence of secondary flow across the cavity thickness, in the vicinity of the front region where the unstable flow develops. Moreover, the unstable flow is confined to a small area in the front region whose width is of the order of the cavity thickness.

A pressure transducer was used to measure the pressure history near the gate throughout flowing. The result is presented in Fig. 12, where we observe a slight non-linearity of the pressure history due to the radial flow at the beginning of the filling. The pressure decrease corresponds to the end of filling.

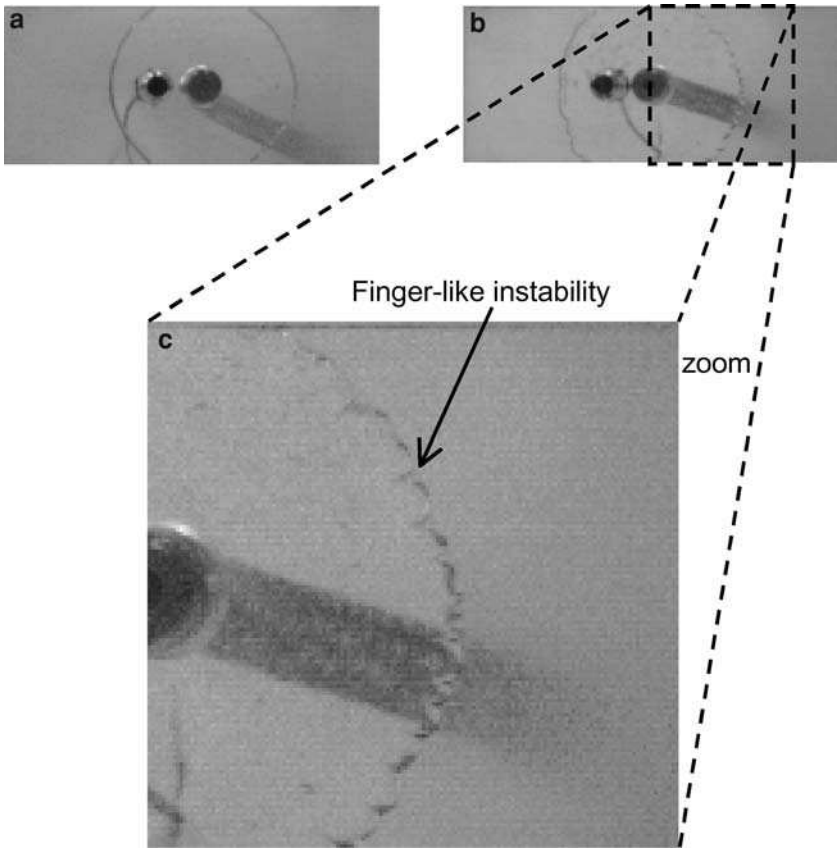

Fig. 9 Effect of PAA ($5–6\times10^6$ g mole^{-1}) concentration, c, on the flow-front fingering instabilities during filling: **a** the nearly inelastic PAA solution with $c=0.015\%$, **b, c** the PAA Boger fluid with $c=0.1\%$

Similar results are also obtained with the PIB Boger fluid consisting of 0.1% by weight of PIB, 92.1% of PB and 7.8% of kerosene. The flow-front results at two different times during flowing are presented in Fig. 13. As in the experiments with the 0.1% PAA Boger fluid, the same instabilities at the flow-front are observed. Therefore, definitive conclusions may be drawn about the existence of such an elastic flow-front fingering instability.

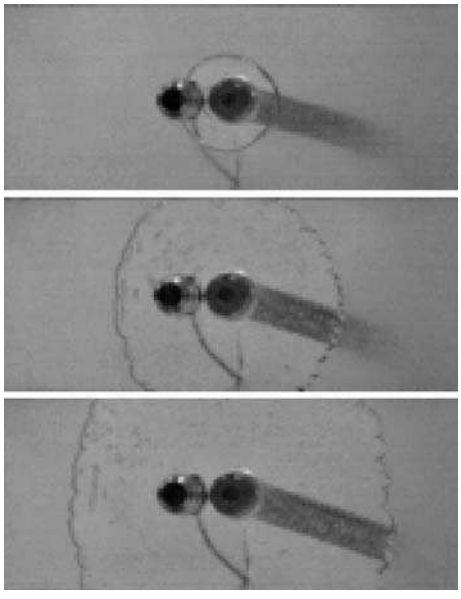

Fig. 10 Flow-front patterns at different times during filling for the PAA Boger fluid: 0.1% by weight solution of PAA in the mixture of corn syrup (95%) and water (5%)

The effect of molecular weight on the occurrence of the flow-front instability is further analyzed in Fig. 14 for two solutions: the 0.1% by weight of a low molecular weight PAA (10^4 g/mole) solution, in the mixture of corn syrup (95%) and water (5%); and the 0.1% PAA Boger fluid (previously studied). While a smooth flow-front pattern is observed in Fig. 14a for the 0.1% low molecular weight PAA solution (Newtonian fluid), finger-like pattern is exhibited in Fig. 14b for the high molecular weight PAA Boger fluid.

A question that is raised from these observations is, 'Under what conditions finger patterns occur at the advancing flow-front?' Let us analyze closely the mechanism of such an elastic flow-front instability. To determine the onset conditions of the occurrence of the unstable flow at the front region, we carried out a series of 1-D filling experiments of the rectangular Hele-Shaw cell through a rectilinear gate, in which the initial flow-front shape was rectilinear in the middle-plane. The shear rate is estimated as $\dot{\gamma}=\bar{v}_f/h$, with h the cavity

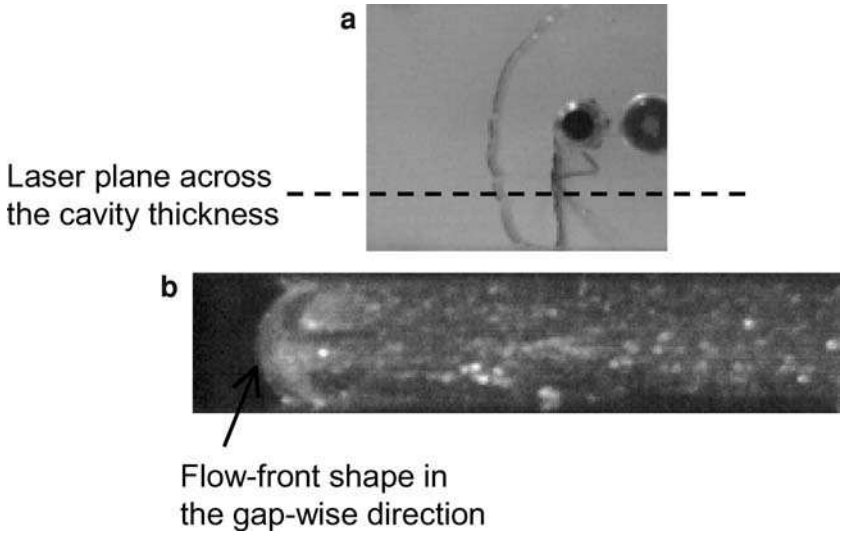

Fig. 11 Flow-front shape in two different planes at a given time during filling for the 0.1% PAA Boger fluid: **a** Flow-front shape in the middle-plane, and **b** Flow-front shape across the cavity thickness (gap-wise direction) by means of the laser sheet lighting across the cavity thickness

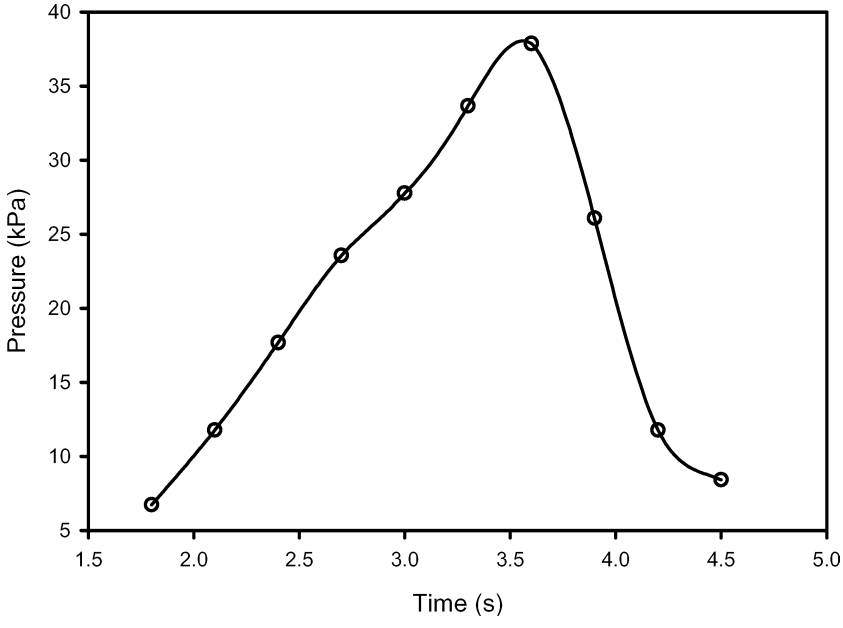

Fig. 12 Pressure history near the gate during filling for the 0.1% PAA Boger fluid

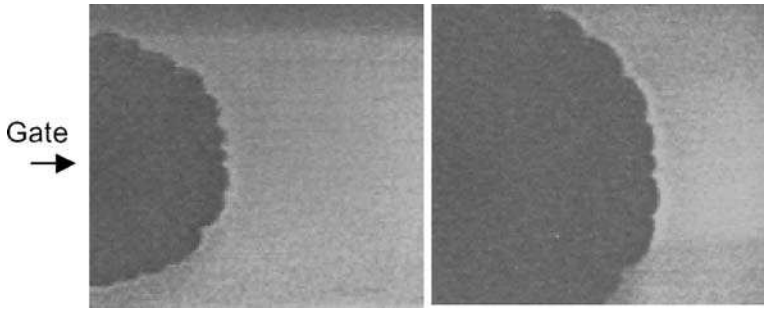

Fig. 13 Flow-front patterns at two different times during filling for the PIB Boger fluid consisting of 0.1% by weight of PIB, 92.1% of PB and 7.8% of kerosene

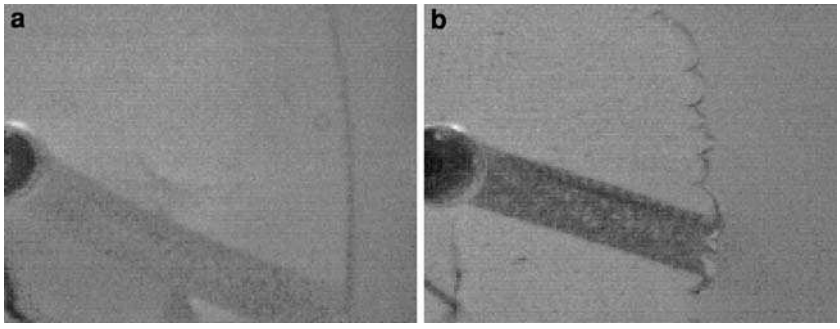

Fig. 14 Effect of the molecular weight, M_w, on the flow-front fingering instabilities: **a** 0.1% PAA, $M_w = 10{,}000$ g mole^{-1} (inelastic fluid) in the mixture of corn syrup (95%) and water (5%), and **b** 0.1% PAA Boger fluid $M_w = 5$–6×10^6 g mole^{-1} in the same mixture

thickness, and $\bar{v}_f$ the average flow-front velocity. It should be noted that the shear rate is nonuniform throughout the fluid. Nevertheless, it should provide a reasonable indication of the maximum shear rate that is encountered in these experiments. We further define the Weissenberg number, We, as

$$\mathrm{We} = \lambda_p \dot{\gamma}$$

By increasing progressively the flow rate in our 1-D filling experiments, we noted that for the 0.1% PAA Boger fluid the critical condition was roughly $\dot{\gamma}_c = 0.33\,\mathrm{s}^{-1}$ ($h = 2$ mm and $\bar{v}_f = 0.66$ mm/s), which corresponds to $\mathrm{We}_c = 23$ and $\lambda_p = 70$ *s*, as estimated from measurements of the normal stress decay on cessation of steady shear flow (Fig. 8). The critical condition in the rectangular Hele-Shaw cell corresponds to the shear rate at which we observe an unstable flow at the flow-front region, characterized by the occurrence of finger patterns. We therefore re-analyze the transient response of the shear stress (Fig. 6) and the first normal stress difference (Fig. 7) in the plate-and-plate geometry, above the critical condition ($\dot{\gamma}_c = 0.33\,\mathrm{s}^{-1}$) for the elastic fingering instability in the Hele-Shaw cell. The transient response above critical did not reveal any flow transition or rapid changes of the elastic properties that might be related to the finger pattern instability found in the rectangular Hele-Shaw cell. In addition, at critical condition for the occurrence of finger patterns in the Hele-Shaw cell, the small induction time for the instability (about 300 ms) suggests that the unstable flow at the flow-front develops prior to the overshoot of the transient response in the plate-and-plate geometry, as highlighted in Figs. 6, 7. Furthermore, above that critical shear rate (in the range of the shear rate investigated) we did not observe any irregular distortions of the meniscus in the plate-and-plate geometry. What our results show, however, is that at critical condition the unstable flow in the Hele-Shaw cell is only confined to a small area in the front region whose width is of the order of the cavity thickness, although the behavior of the main flow, upstream of the flow-front, is stable and parallel to the walls (Fig. 11b), consistent with the results in the plate-and-plate geometry which show no transition or irregular distortion of the meniscus at that critical condition for the elastic fingering instability in

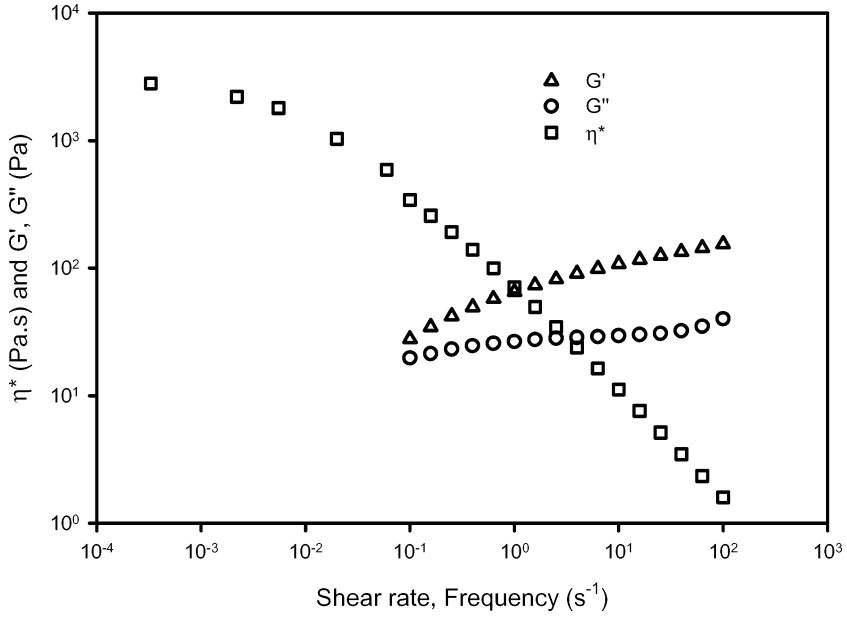

Fig. 15 Complex viscosity, η^*, storage and loss moduli, G' and G'', as a function of frequency at 23 °C for the 3.5% PAA aqueous solution

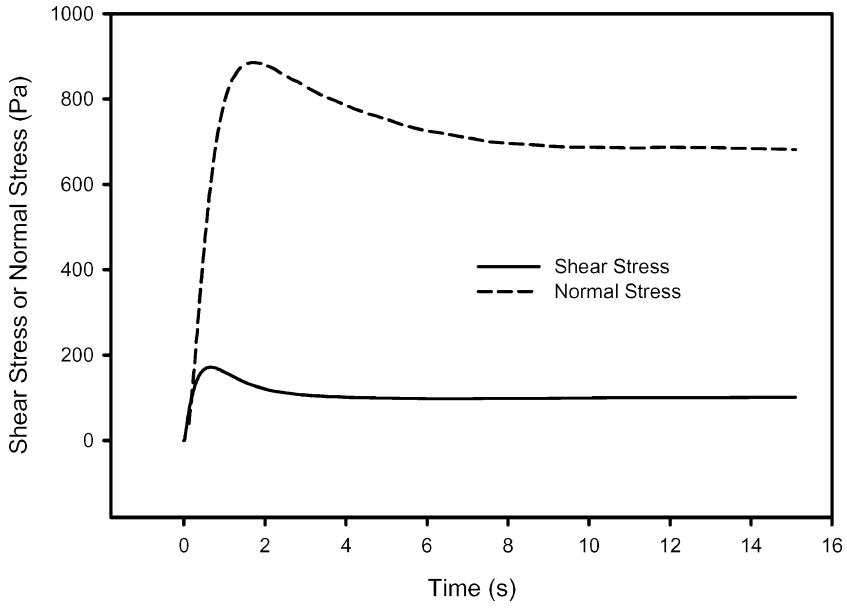

Fig. 16 Time dependence of the shear stress and the first normal stress difference, N_1, in the plate-and-plate geometry at $\dot{\gamma} = 6\,s^{-1}$ for the 3.5% PAA aqueous solution

the Hele-Shaw cell. It follows from our experimental results that the elastic flow-front instability in the rectangular Hele-Shaw cell occurs at shear rate that is relatively much smaller ($\dot{\gamma}_c = 0.33\,s^{-1}$) than the critical shear rate ($\dot{\gamma}_c = 4\,s^{-1}$) at which a flow transition or an irregular distortion of the meniscus is observed in the plate-and-plate geometry.

To explain the origin of this instability we invoke the interaction between the gradient of the normal stress difference and the free surface (advancing flow-front). Our experimental observation has shown that at critical shear rate, the main flow upstream of the flow-front remains stable and parallel to the walls, whereas trajectories are strongly perturbed in the vicinity of the advancing flow-front. Hence, the flow in the front region is partly an elongational flow and partly a shear flow, while the shear rate is nonuniform throughout the solution. Thus, the normal stress difference exerts an extra pressure in the shear direction that depends on the local shear rate within the solution. The calculated critical shear rate in the rectangular Hele-Shaw cell is about 0.33 s^{-1}, which is greater than the inverse relaxation time $\lambda_p^{-1} = 0.014\ s^{-1}$ of the PAA Boger fluid, indicating that elastic effects in the fluid become significant. We suggest that the origin of finger patterns at the advancing flow-front is associated with gradients of extra pressure that normal stress difference exerts in the fluid, although at that critical condition the main flow remains stable.

Another question that is raised from these observations is; 'Why at critical condition the flow-front exhibits finger patterns only in the middle-plane direction and not across the cavity thickness plane?' (Fig. 11). A possible explanation is the narrow gap (3 mm or 6 mm) of the Hele-Shaw cell used in the filling experiments.

Shear thinning viscoelastic fluid: PAA aqueous solution

Finally, in a last series of experiments, a purely aqueous solution consisting of 3.5% by weight PAA ($5–6\times10^6$ g $mole^{-1}$) in water, were designed. The rheological characterizations of this solution are shown in Figs. 15, 16. It can be seen from Fig. 15 that the 3.5% PAA aqueous solution shear thins in viscosity at shear rate of about $10^{-3}\ s^{-1}$. The results for the storage modulus, G', and the loss modulus, G'', in oscillatory shear are presented in Fig. 15, and those for the normal stress difference and the shear stress upon the inception of steady shear flow are shown in Fig. 16. The polymeric relaxation time, λ_p, for the 3.5% PAA aqueous solution has been determined from measurements of the normal stress decay on

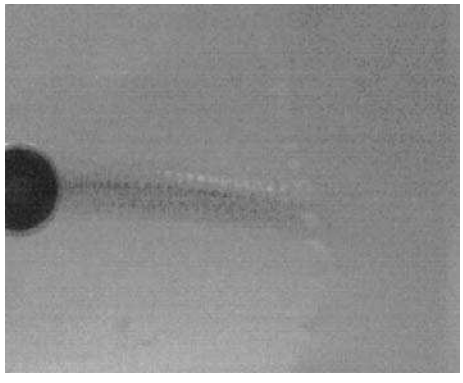

Fig. 17 Flow-front pattern during filling for the 3.5% PAA ($M_w = 5–6\times10^6$ g $mole^{-1}$) aqueous solution (shear thinning viscoelastic fluid)

cessation of steady shear flow at shear rate $\dot{\gamma} = 6\,s^{-1}$ and yields an estimate of about $\lambda_p = 2$ s (much smaller than λ_p for the PAA Boger fluid; about 70 s). Figure 17 presents the flow-front pattern at a given time during filling. The preceding flow-front instabilities are still observed and are only confined in the flow-front region. The critical condition was roughly $\dot{\gamma}_{crit} = 5\,s^{-1}$, which is greater than the inverse relaxation time $\lambda_p^{-1} = 0.5\ s^{-1}$ of the 3.5% shear thinning PAA fluid. As in the preceding experiments for the Boger fluids, transient response in the plate-and-plate geometry, above critical for the elastic fingering instability in the Hele-Shaw cell, did not reveal any flow anomalous or irregular distortions of the meniscus.

Finally, we note that the PAA Boger fluid exhibits fingering instabilities at a critical shear rate ($\dot{\gamma}_c = 0.33\,s^{-1}$) much smaller than the critical ($\dot{\gamma}_{crit} = 5\,s^{-1}$) for the PAA viscoelastic shear thinning fluid.

Remarks

Macroscopic flow visualization experiments were conducted to elucidate flow-front fingering instabilities that occur during the flowing of polymer solutions in an empty mold cavity. Mechanisms that produce those instabilities are explained. The instability studied in this work differs from others instabilities reported previously in the literature:

1. Purely viscous instability: experiments using a rectangular Hele-Shaw cell and involving polymer solutions (Newtonian or non-Newtonian), in which a more viscous fluid is penetrated by a less viscous one revealed complex fingering patterns. As previously mentioned, this is referred to as a Saffman-Taylor or viscous fingering instability. The mechanisms involved in those flows are extensively studied in the literature (see, e.g., Kondic et al. 1998; Linder et al. 2000, 2002; Fast et al. 2001) and differs from the one reported in this work. In the present study, the air in the cavity is continuously evacuated to avoid any compressive effect. Thus, the fingering instability reported here is a consequence of the sole elasticity of the solution.
2. Elastic instability: Magda and Larson (1988) reported a transition occurring in ideal elastic liquids during shearing flows. They found a time-dependent increase in the elasticity and the shear viscosity or anti-thixotropic behavior above a critical shear rate that depends upon molecular weight and shearing time. They concluded that this transition is a manifestation of an instability predicted by Phan-Thien (1983, 1985) for the Oldroyd-B constitutive equation in cone-plate and parallel-plate geometries above a critical Weissenberg number. McKinley et al. (1991) also reported observations on the elastic instability in cone-and-plate and parallel-plate flows of a PIB Boger fluid. They demonstrated the presence of a time-dependent transition or anti-thixotropic behavior. Finally, Grillet et al. (2002) investigated numerically the stability of injection molding flow to elucidate the mechanism of flow mark surface defects. They used a single mode exponential Phan-Thien-Tanner constitutive equation, along with a linear stability analysis to determine the most unstable mode of the flow. The difference between the Phan-Thien elastic instability and the one we observed is that the transient response in the plate-and-plate geometry, above the critical condition for the elastic fingering instability in the Hele-Shaw cell, did not reveal any flow transition or rapid changes of the elastic properties that might be related to the finger pattern instability found in the rectangular Hele-Shaw cell. Furthermore, above that critical shear rate we did not observe any irregular distortions of the meniscus in the plate-and-plate geometry. The unstable flow at the advancing flow-front in the Hele-Shaw cell observed in this study manifests at critical shear rate that is much below the critical for the flow transition in the plate-and-plate or cone-and-plate geometry.

Finally, we wish to mention that most of the numerical modeling studies in injection molding are based on the lubrication approximation to formulate the mold filling problems (see, e.g., Williams and Lord 1975; Hieber and Shen 1980; Dupret and Vanderschuren 1988; Chiang et al. 1991; Dupret et al. 1999), although a number of recent papers use a fully three-dimensional approach (see, e.g., Pichelin and Coupez 1999; Ilinca and Hétu 2001; Michaeli et al. 2001) to address specific problems that need to solve the full Navier-Stokes equations. Nevertheless, all published theoretical studies and simulations are far from predicting flow-front finger-like instabilities described in this study due to the lack of physics in the models used.

Conclusions

Our experimental results have shown the existence of an elastic instability that develops at the advancing flow-front of ideal elastic Boger fluids and shear thinning viscoelastic fluids, in an empty mold cavity, with an onset time of a few hundred milliseconds. The unstable flow seems to be confined to a small area in the front region whose width is of the order of the cavity thickness although the main flow upstream the flow-front remains stable. This elastic instability manifests at critical shear rate that is much smaller than the critical for the flow transition in the plate-and-plate or cone-and-plate geometry. We suggest that the extra

pressure that the normal stress difference exerts in the shear direction is responsible of the finger patterns developed at the advancing flow-front. We wish to point out that such an elastic flow-front instability is not at all chaotic; instead fingers appear and grow up to a point, and then their amplitude and number remain roughly constant in the course of the rest of the filling.

References

Cahn JW, Hilliard JE (1958) Free energy of a nonuniform system I. Interfacial free energy. J Chem Phys 28:258–267

Chen CY, Wang L, Meiburg E (2001) Miscible droplets in a porous medium and the effects of Korteweg stresses. Phys Fluids 13:2447–2456

Chiang HH, Hieber CA, Wang KK (1991) A unified simulation of the filling and postfilling stages in injection molding. Part I: Formulation. Polym Eng Sci 31:116–124

Denn MM (2001) Extrusion instabilities and wall slip. Annu Rev Fluid Mech 33:265–287

Dupret F, Vanderschuren L (1988) Calculation of the temperature field in injection molding. AIChE J 4:1959–1972

Dupret F, Couniot A, Mal O, Vanderschuren L, Verhoyen O (1999) Modelling and simulation of injection molding. In: Siginer DA, De Kee D, Chhabra RP (eds) Rheology Series. Advances in the flow and rheology of non-Newtonian fluids. Elsevier, Amsterdam, pp 939–1010

Fast P, Shelley MJ, Palffy-Muhoray P (2001) Pattern formation in non-Newtonian Hele-Shaw flow. Phys Fluids 13:1191–1212

Grillet AM, Bogaerds ACB, Peters GWM, Baaijens FTP (2002) Numerical analysis of flow mark surface defects in injection molding flow. J Rheol 46:651–669

Hieber CA, Shen SF (1980) A finite element/finite-difference simulation of the injection molding filling process. J Non-Newtonian Fluid Mech 7:1–32

Ilinca F, Hétu JF (2001) Three-dimensional filling and post-filling simulation of polymer injection molding. Int Polym Process 16:291–301

Jackson KP, Walter K, Williams RW (1984) A rheometrical study of Boger fluids. J Non-Newtonian Fluid Mech 14:173–188

Kabanemi KK, Gobeaux JP (1987) Étude expérimentale et théorique du moulage par injection. Mechanical Engineering Dissertation, MEMA, Université Catholique de Louvain, Belgium

Kondic L, Shelley MJ, Palffy-Muhoray P (1998) Non-Newtonian Hele-Shaw flow and Saffman-Taylor instability. Phys Rev Let 80:1433–1436

Larson RG (1992) Instabilities in viscoelastic flows. Rheologica Acta 31:213–263

Larson RG, Shaqfeh ESG, Muller SJ (1990) A purely elastic instability in Taylor-Couette flow. J Fluid Mech 218:573–600

Linder A, Bonn D, Meunier J (2000) Viscous fingering in a shear-thinning fluid. Phys Fluids 12:256–261

Linder A, Bonn D, Poiré EC, Ben Amar M, Meunier J (2002) Viscous fingering in non-Newtonian fluids. J Fluid Mech 469:237–256

Magda JJ, Larson RG (1988) A transition occurring in ideal elastic liquids during shear flow. J Non-Newtonian Fluid Mech 30:1–19

McKinley GH, Byars JA, Brown RA, Armstrong RC (1991) Observations on the elastic instability in cone-and-plate and parallel-plate flows of a polyisobutylene Boger fluid. J Non-Newtonian Fluid Mech 40:201–229

Michaeli W, Hoffmann S, Kratz M, Webelhaus K (2001) Simulation opportunities by a three-dimensional calculation of injection moulding based on the finite element method. Int Polym Process 16:398–403

Petrie CJS, Denn MM (1976) Instabilities in polymer processing. AIChE J 22:209–236

Phan-Thien N (1983) Coaxial-disk flow of an Oldroyd-B fluid: exact solution and stability. J Non-Newtonian Fluid Mech 13:325–340

Phan-Thien N (1985) Cone-and-plate flow of the Oldroyd-B fluid is unstable. J Non-Newtonian Fluid Mech 17:37–44

Pichelin E, Coupez T (1999) A Taylor discontinuous Galerkin method for the thermal solution in 3D mold filling. Comput Methods Appl Mech Eng 178:153–169

Williams G, Lord HA (1975) Mold-filling studies for injection molding of thermoplastic materials: Part I: The flow of plastic materials in hot- and cold-walled circular channels. Polym Eng Sci 15:553–568